

Mass transfer study using an electrochemical method

M.A. Cancela*, R. Maceiras, E. Álvarez, X.R. Nóvoa

University of Vigo, Chemical Engineering Department, ETSEI; Rua Maxwell s/n, 36310 Vigo, Spain.

Abstract

The volumetric mass transfer coefficients at different axial positions in a bubble column were measured using a conductivity method. The absorption process of CO₂ in monoethanolamine solutions was carried out in a prismatic column 0.06 m side and 1.03 m height. Measurements were conducted at various gas flow rates and amine concentration. The local mass transfer was found to vary significantly in the axial direction.

Keywords: Local mass transfer coefficient, electrochemical method, carbon dioxide, monoethanolamine, bubble column.

1. Introduction

Many processes in the field of chemical engineering are related to mass transfer operations between different phases, generally gas and liquid phases. One of the most important is the removal of acid gases, such as H₂S and CO₂ from natural and industrial exhausts using alkanolamine solutions. Among the industrially important alkanolamines, the primary amines such as the monoethanolamine (MEA) are the most employed.

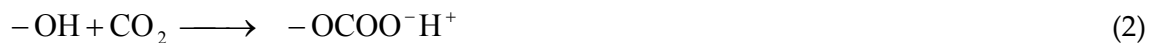
More stringent regulations governing the emission of toxic gases from industrial sources have evoked an increasing demand for new and efficient abatement techniques. In the last years, different electrochemical methods have been used to study the mass transfer, measuring the mass transfer coefficient in different equipments (Kleifges *et al.*, 1997; Vilar and Coeuret, 1999; Oduoza and Wragg, 2000; Coueret, 2001; Gostick *et al.*, 2003; Verma and Rai, 2003; Arzutug *et al.*, 2005; Dang-Vu *et al.*, 2006a,b; Han and Al-Dahhan, 2007).

In this work, the application of an electrochemical method to directly measure local mass transfer coefficients during the removal of carbon dioxide using monoethanolamine aqueous solutions is discussed. This method overcomes some of the shortcomings inherent to other techniques since it permits mass transfer coefficients to be directly determined from the

measurement of local conductivity changes. Two requirements must be considered in order to analyze the absorption process by means of conductivity measurements. On the one hand the thorough contact between the gas and the absorbent liquid (to transfer the reactant from the gas phase to the liquid phase); and on the other hand the thorough contact between the liquid phase and the metallic electrode (which drives the necessary electric current through the system). Considering these requirements, a bubble column with electrodes distributed along the reactor walls was designed. This approach can be easily extended in future work to investigate the effect of other factors.

2. Theory

Monoethanolamine (MEA) solution is an important solvent in the CO₂ removal process because it reacts quickly with carbon dioxide for its primary amine characteristics. The monoethanolamine, H₂N-CH₂-CH₂-OH, is a primary amine in which the nitrogen atom is bonded to an ethanol group, and both the amine group ($-\overset{|}{\text{N}}\text{H}$) and the alcohol group ($-\text{OH}$) can react with CO₂ to produce carbamic acid (Eq. 1) and carbonic acid (Eq. 2) (Astarita *et al.*, 1964; Clarke, 1964; Hart, 1976; Hikita *et al.*, 1977a,b; Álvarez-Fuster *et al.*, 1980; Deckwer, 1980; Camacho *et al.*, 2000; Dhotre *et al.*, 2005; Verma, 2005):



The carbonic acid formation may take place in alkaline solution at a pH ≥ 11 . Nevertheless, for pH < 10 , even in a carbonate solution, the formation of the carbonic-acid derivative can be considered negligible (Astarita *et al.*, 1964). Measurements indicate that, in our experiments, the pH was less than 11 from the beginning of the absorption process and decreased gradually during the process. On the basis of the results obtained, the main reaction can be considered to be the formation of a carbamic-acid derivative (Eq. 1).

On the other hand, the reaction regime between CO₂ and MEA solutions is instantaneous (Clarke, 1964; Hikita *et al.*, 1977a,b; Álvarez-Fuster *et al.*, 1980). In this case, the rate of absorption of carbon dioxide per unit volume, R_A , is computed from the following expression:

$$R_A = k_L a \cdot C_A^* \left(1 + \frac{D_B}{z \cdot D_A} \cdot \frac{C_{B0}}{C_A^*} \right) \quad (3)$$

Therefore, the volumetric mass transfer coefficient, $k_L a$, can be obtained as follows:

$$k_L a = \frac{R_A}{C_A^* \left(1 + \frac{D_B}{z \cdot D_A} \cdot \frac{C_{B0}}{C_A^*} \right)} \quad (4)$$

where C_A^* is the gas solubility ($\text{kmol}\cdot\text{m}^{-3}$), z is the stoichiometric coefficient, D_A and D_B are the diffusivities of CO_2 and MEA in aqueous monoethanolamine solutions, respectively, ($\text{m}^2\cdot\text{s}^{-1}$) and C_{B0} is the bulk initial concentration of the amine ($\text{kmol}\cdot\text{m}^{-3}$).

3. Experimental

3.1. Materials and methods

The experimental setup is shown in Fig. 1. A bubble column was used in this work for the absorption of CO_2 into aqueous monoethanolamine solutions. Absorption measurements were performed at room temperature, operating in batches with respect to the liquid phase. The bubble column is made of methacrylate, 1.03 m height, and has a square cross-section (side length 6 cm). For the injection and uniform distribution of the gas phase, a gas sparger, i.e., a porous plate of 4 mm in diameter is installed at the centre of the bottom plate. This plate has another orifice for liquid outlet. There are also three orifices at the top plate: liquid inlet, gas outlet and a thermometer.

Each experimental run was started by filling the column with the liquid phase up to 100 cm above the sparger. Carbon dioxide, saturated with water vapour at ambient temperature (22 ± 2 °C), was fed through the bottom of the bubble column. The gas flow, before entering the bubble column, was metered by a flow meter and controlled with a flow controller (Brooks model 0154). The gas pressure was measured in the inlet using a digital manometer (Testo model 512). The gas flow in the outlet was measured with a soap meter. The gas absorption rate was calculated as the difference between the flow rates gas into and out of the bubble column.

The electrical circuit consists of a function generator working at 1 kHz (sine wave) connected through a switching box in series with a standard resistor and each of the electrode pair in the column. The 1 kHz frequency was chosen from previous calibration in order to overcome the electrode's polarization resistance. A high impedance AC voltmeter measures the current flux through the standard resistor, which is inversely proportional to the ohmic drop for each electrode pair. The geometry of the electrodes is chosen so that voltmeter readings correspond directly to electrolyte resistivity (in $\Omega\cdot\text{cm}$).

Local mass transfer coefficients were determined under different conditions at 5 axial

levels in the column. The axial levels were 22 cm apart, starting 10 cm above the gas distributor. At each axial level, two AISI316 stainless steel sheets were arranged in two opposite faces to be used as the sensing electrodes. The lateral faces of the steel sheets were coated with cataphoretic paint so that only the front part of the electrode contacts the electrolyte. The steel sheets were fixed to the column by steel screws also insulated with the cataphoretic paint.

Aqueous monoethanolamine (MEA) solutions of different concentrations were employed as liquid phase, while the gas phase was carbon dioxide. Different gas flow rates for each run were selected. The amine concentrations were varied between 0 and 1.0 M. Gas flow rates were varied between 10 and 25 L/h to study the effect of the gas flow rate on mass transfer coefficients. In all experiments the volume of liquid has been constant and equal to 3.6 L.

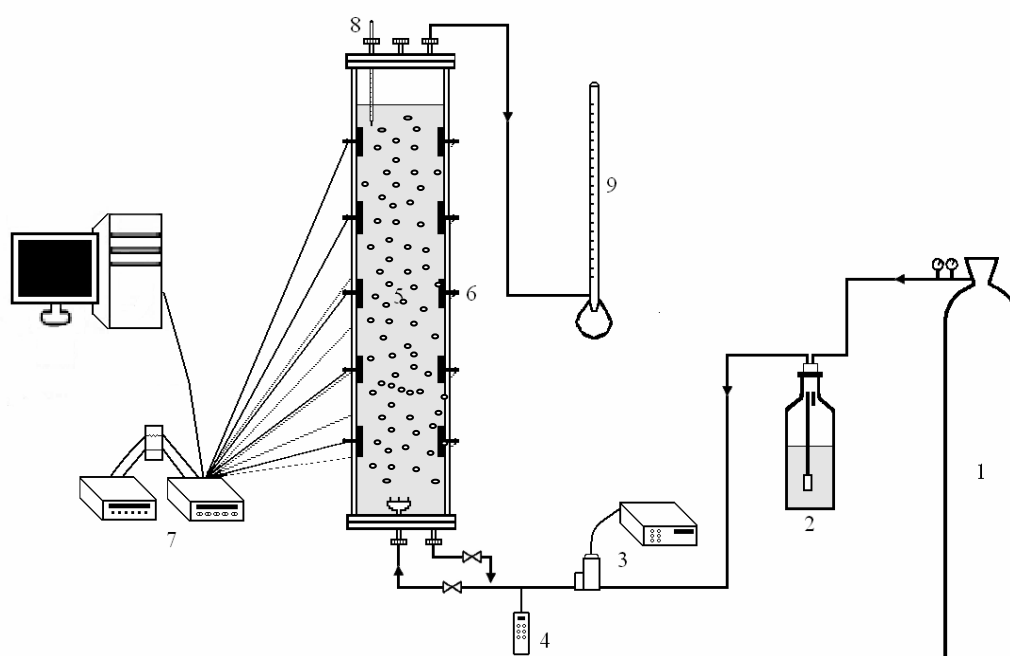


Figure 1. Schematic figure of the bubble column reactor: (1) pressurized CO₂ source, (2) humidifier, (3) flow-meter / regulator, (4) digital manometer, (5) bubble column, (6) stainless steel (SS-316) electrodes, (7) electronic and electrical equipment for local resistance measurement, (8) thermometer, (9) output flow-meter.

3.2. Physical Properties

The interpretation and correlation of the experimental mass-transfer data require knowledge of the physical properties of the liquid phases as well as the gas solubilities and diffusivities in these phases.

The densities, ρ , and viscosities, μ , were measured at 20, 25 and 30 °C using a Anton

Paar DSA 5000 densimeter, with a precision of $\pm 10^{-5} \text{ g}\cdot\text{cm}^{-3}$, and a Shott-G eratte AVS 350 automatic viscometer, with a precision of $\pm 0.01 \text{ s}$, respectively. The experimental values were correlated simultaneously with the amine concentration. The values are reported in Maceiras *et al.* (in press). The solubilities and diffusivities of the CO_2 and MEA were calculated using the correlation equations found in the literature (Wilke and Chang, 1955; Danckwerts, 1970; Sada *et al.*, 1978; Versteeg *et al.*, 1987; Versteeg and Van Swaaij, 1988).

4. Results and Discussion

Mass transfer coefficients can be obtained through conductivity measurements because CO_2 reacts with the MEA producing ionic species. All the details about the data acquisition are reported in Maceiras *et al.* (in press).

The plot in Fig. 2 shows the variation of the absorption rate (obtained through conductivity measurements) with the time, at different axial positions. It can be observed that in the beginning the absorption process occurs initially at the bottom of the column while in the upper part absorption begins only about 20 minutes later. This fact, evident from Fig. 2 data is due to the reaction regime: when CO_2 enters the column, the reaction occurs instantaneously and the amount of carbon dioxide that rises in the column lies out of the detection limit.

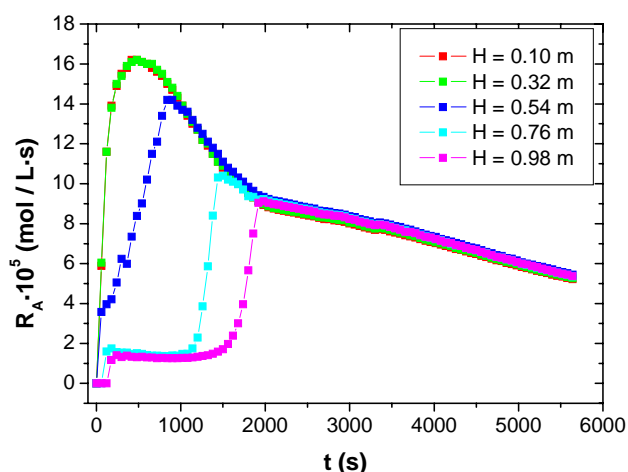


Figure 2. Variation of the absorption rate with the time for MEA 0.3 M and $25 \text{ L}\cdot\text{h}^{-1}$.

Once the absorption rate has been obtained, the local volumetric mass transfer coefficients were calculated using the Eq. (4) for all the amine concentrations and gas flow rates. The effect of the gas flow rate is presented in Fig. 3, where the Reynolds number is employed to quantify flow rate. Thus, the effect of the electrode-to-sparger distance (H/d) is explored. As expected (from Fig. 2 data), the mass transfer coefficients decrease considerably with

increasing (H/d) and $k_L a$ values increase with the Reynolds number at a given axial position.

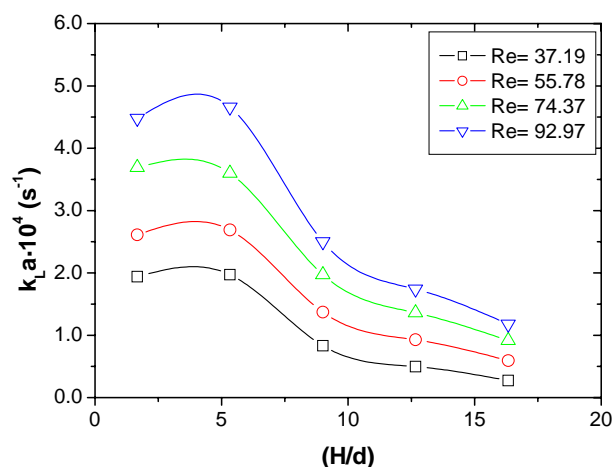


Figure 3. Local mass transfer coefficient for different Re and amine concentration of 1 M.

5. Conclusions

In this work, an electrochemical technique has been used to measure the local mass transfer coefficients. The results obtained suggest that the assumption of a constant mass transfer coefficient throughout the bubble column is erroneous and may lead to important errors in designing and scaling up bubble columns, since the local mass transfer coefficient varies with the axial position.

References

- Álvarez-Fuster, C., Midoux, N., Laurent, A., Charpentier, J.C., (1980) *Chemical Engineering Science*, 35, 1717-1723.
- Arzutug, M. E., Yapici, S., Muhtar Kocakerim, M., (2005) *International Communications in Heat and Mass Transfer*, 32, 842–854.
- Astarita, G., Marrucci, G., Gioia, F., (1964) *Chemical Engineering Science*, 19, 95-103.
- Camacho, F., Sánchez, S., Pacheco, R., (2000) *Chemical Engineering & Technology*, 23, 1073-1080.
- Clarke, J.K.A., (1964) *Industrial & Engineering Chemistry Fundamentals*, 3, 239-245.
- Couret, F., (2001) *Journal of Applied Electrochemistry*, 31, 193-199.
- Dankwerts, P.V., *Gas Liquid Reactions*. McGraw-Hill, London (1970).
- Dang-Vu, T., Doan, H.D., Lohi, A., (2006a) *Industrial & Engineering Chemistry Research*,

45, 1097-1104.

Dang-Vu, T., Doan, H.D., Lohi, A., Zhu, Y., (2006b) *Chemical Engineering Journal*, 123, 81-91.

Deckwer, W.D., (1980) *Chemical Engineering Science*, 35, 1341-1346.

Dhotre, M.T., Vitankar, V.S., Joshi, J.B., (2005) *Chemical Engineering Journal*, 108, 117-125.

Gostick, J., Doan, H. D., Lohi, A., Pritzker, M. D. (2003) *Industrial & Engineering Chemistry Research*, 42, 3626-3634.

Han, L. M., Al-Dahhan, H., (2007) *Chemical Engineering Science*, 62, 131-139.

Hart, W.F., (1976) *Industrial & Engineering Chemistry Process Design and Development*, 15, 109-114.

Hikita, H., Asai, S., Ishikawa. H., Honda, M., (1977a) *Chemical Engineering Journal*, 13, 7-12.

Hikita, H., Asai, S., Ishikawa. H., Honda, M., (1977b) *Chemical Engineering Journal*, 14, 27-30.

Kleifges, K-H., Kreysa, G., Juëttner, K., (1997) *Journal f Applied Electrochemistry*, 27, 1012-1020.

Maceiras, R., Cancela, M.A., Álvarez, E., (in press) *Chemical Engineering Journal*.

Maceiras, R., Nóvoa, X.R., Álvarez, E., Cancela, M.A., (in press) *Chemical Engineering & Processing*.

Oduoza, C.F., Wragg, A.A., (2000) *Journal of Applied Electrochemistry*, 30, 1439-1444.

Sada, E., Kumazawa, H., Butt, M.A., (1978) *Journal of Chemical & Engineering Data*, 23, 161-163.

Verma, A.K., (2005) *Industrial & Engineering Chemistry Research*, 41, 882-884.

Verma, A.K., Rai, S., (2003) *Chemical Engineering Journal*, 94, 67-72.

Versteeg, G.F., Blauwhoff, P.M.M, van Swaaij, W.P.M., (1987) *Chemical Engineering Science*, 42, 1103-1109.

Versteeg, G.F., Van Swaaij, W.P.M., (1988) *Journal of Chemical & Engineering Data*, 33, 29-34.

Vilar, E.O., Coeuret, F., (1999) *The Canadian Journal of Chemical Engineering*, 77, 855-862.

Wilke, C.R., Chang, P., (1955) *AIChE Journal*, 1, 264-270.